ISBN: 978-3-95450-212-7 ISSN: 2673-5482 doi:10.18429/JACoW-CYCLOTRONS2022-WEPO018

PROGRESS IN THE DESIGN OF A NEW 150-MHz FLAT TOP CAVITY FOR THE PSI RING CYCLOTRON

J.-Y. Raguin*, M. Bopp, R. Fortunati, J. Grillenberger, T. G. Lucas, M. Pedrozzi,
M. Schneider, M. Stoll, Paul Scherrer Institut, 5232 Villigen PSI, Switzerland
E. Solodko, Transmutex SA, 1214 Vernier, Switzerland

Abstract

Increasing PSI's 590-MeV main cyclotron beam current to 3 mA requires the replacement of the existing power-limited 150-MHz flat top cavity with a new cavity. This new cavity has been designed to withstand a 700-kV peak voltage and a 140-kW dissipated average power. Although very similar in its geometry to the original flat top cavity currently in operation, in the new design, special attention has been paid to the shaping of the four electrodes for maximizing the shunt impedance. Furthermore, the topology of the cooling water channels has been optimized to increase the power handling capabilities of the cavity. Finally, in order to mitigate multipacting observed in the current design, variations on the new cavity baseline geometry have started to be explored.

INTRODUCTION

The PSI High Intensity Proton Accelerator (HIPA) facility consists primarily of the 72-MeV injector cyclotron (Injector II) and the 590-MeV Ring cyclotron. The Injector II cyclotron is currently being upgraded through the installation of new 50-MHz aluminum cavities designed to withstand a peak voltage of 400 kV and an average dissipated power of 50 kW [1]. The Ring cyclotron has been progressively upgraded with four new copper 50-MHz cavities capable of generating a 1-MV peak voltage and able to dissipate an average power of 500 kW [2]. However, the 150-MHz flat top cavity is currently the limiting feature of the Ring cyclotron [3].

For a 3-mA beam current, each 50-MHz main cavity of the Ring cyclotron requires a peak accelerating voltage of 910 kV. The required peak voltage of the 150-MHz flat top cavity would then be 640 kV [4]. Adding some reserve, the new cavity is being designed for a maximum peak voltage of 700 kV.

RF DESIGN STUDIES

Since the existing mechanical constraints severely limit deviations from the current geometry, the new cavity RF studies performed with the 3D electromagnetic code ANSYS HFSS [5] mainly focused on optimizing the electrodes that protrude into the cavity. Several cavities without RF coupler were designed with electrodes thickness of 45 mm, 55 mm and 65 mm and with a horizontal gap between electrodes ranging from 140 mm to 250 mm, this later distance being considered as maximum to reduce field leakage. The virtual tuning to reach the design frequency of 151.8984 MHz in each of these cavities was done by adjusting the cavity height (along the Z-axis in Fig. 1). The inner maximum length, the inner width and the length of the four electrodes, which are 2700 mm, 200 mm and 2585 mm, respectively, have been kept the same as in the actual cavity. The minimum vertical distance between the electrodes is also the same and is 30 mm. Figure 1 shows one-half of the vacuum volume of the new cavity.

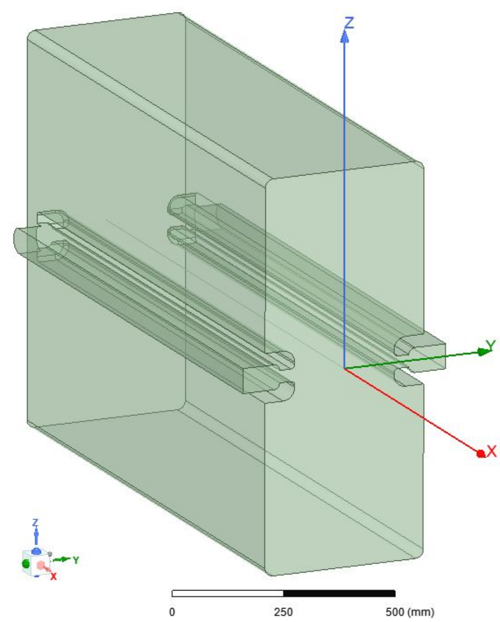

Figure 1: Vacuum volume of the new flat top cavity - One-half shown.

A substantial modification of the cavity consisted in shaping the electrodes to increase the peak shunt impedance R_{sh} ($R_{sh} = V_g^2/P_d$ where $V_g = \int | E_y(0, y, 0) | dy$ is the peak gap voltage and P_d is the power dissipated on the total inner surface). Whereas the tip of the electrodes in the actual cavity is characterized by the single radius 22.5 mm, leading to a maximum electrodes thickness of 45 mm, in the new cavity, the curvature radius closest to the beam plane (XY plane in Fig. 1) was decreased to 10 mm. Such a radius reduction leads to an increase of the shunt impedance. The maximum surface electric field also increases but still stays well below the Kilpatrick limit.

The results of the parametric studies done by varying the horizontal gap between electrodes and the electrode thickness Δz_{elec} are illustrated by Fig. 2. For an aluminum conductivity of 34 MS/m, a peak gap voltage maintained to 700 kV and a gap between electrodes increasing from

* jean-yves.raguin@psi.ch

ISBN: 978-3-95450-212-7	ISSN: 2673-5482	doi:10.18429/JACoW-CYCLOTRONS2022-WEPO018

140 mm to 250 mm, the total dissipated power decreases from about 220 kW to about 130 kW. Moreover, thickening the electrodes leads to an increase of the dissipated power, the effect being clearly more pronounced when the distance between electrodes decreases.

A similar trend is observed when computing the dissipated power per electrode (also Fig. 2). For the same variation of distance between electrodes, the dissipated power per electrode decreases from about 13 kW to about 4 kW, a clear consequence of the reduction of the electrodes' surfaces.

These considerations lead to the adoption of an inner volume baseline geometry where the horizontal inter-electrode distance is 250 mm and the thickness of the electrodes is 45 mm.

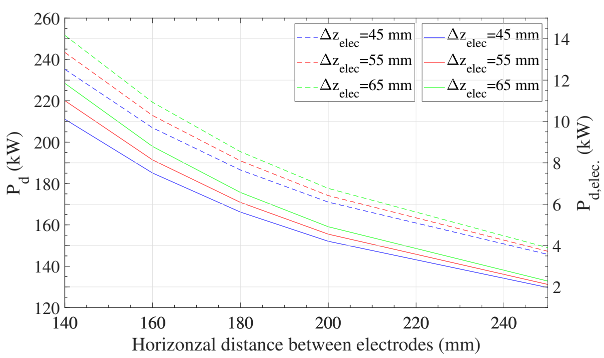

Figure 2: Cavity dissipated power P_d (——) and dissipated power per electrode $P_{d,elec.}$ (- - -) vs. horizontal distance between electrodes and electrode thickness Δz_{elec}.

MECHANICAL DESIGN

The goal of the mechanical design is to define a mechanical structure with a cooling channel system able to keep a relatively low and homogeneous temperature and, consequently, a reasonable deformation of the cavity body to minimize the required range of the tuning system. Within the ANSYS platform Workbench [6], a two-stage approach has to be used:

- One-way analysis defining the temperature distribution and the corresponding structural deformation (HFSS → Steady State Thermal → Static Structural).
- Feedback analysis to evaluate the impact of the deformation on the frequency using the results from the first stage as an input for another iteration of HFSS.

Due to the asymmetry of the mechanical structure of the cavity, the full internal volume (cavity and adjacent vacuum chamber) was simulated with HFSS.

In HFSS, the power dissipated on the outer surface of the vacuum volume has been retrieved. As it is the same surface as the internal surface of the cavity body, results could be imported as Heat Flux (W/m^2) in the ANSYS Steady State Thermal module. Figure 3 shows this imported heat flux map. Note that to simplify the simulations the region of the cavity where the coupler is located (middle of the cavity's top) has been closed by the same material than the rest of the body. A dedicated study with the RF coupler shall be done at a latter stage.

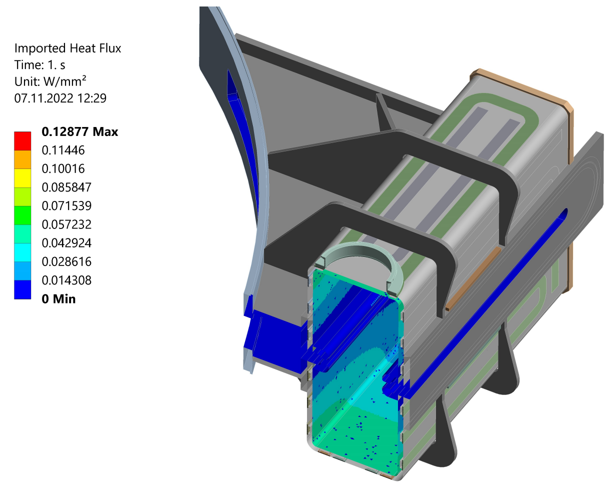

Figure 3: Imported heat flux on the new flat top cavity surface including the adjacent vacuum chamber.

The convection heat transfer coefficient for the forced convection derives from the Dittus-Boelter equation [7] and is 4986 W/(m^{2}K). The water velocity inside the cooling channels (10 mm × 40 mm) is set to 1.2 m/s. This value derived from considerations about possible cavitation and consequently corrosion problems. Higher values of velocity, up to 1.5 m/s, could be considered but do not significantly decrease the temperature. The ambient temperature value is 26 °C and is the temperature inside the HIPA bunker. Air convection coefficient is also considered in the setup and is 10 W/(m^{2}K). The calculated temperature distribution in the flat top cavity body, represented in Fig. 4, has a maximum temperature of 70 °C.

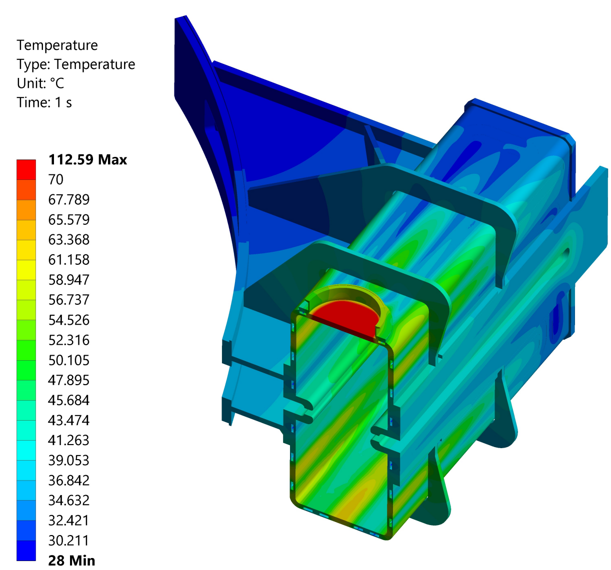

Figure 4: Temperature distribution in the body of the new flat top cavity.

ISBN: 978-3-95450-212-7 ISSN: 2673-5482 doi:10.18429/JACoW-CYCLOTRONS2022-WEPO018

The cooling water temperature varies from 28 °C to 39 °C which gives a temperature difference of 11 °C. These values are acceptable for the existing PSI cooling scheme.

The loads in the ANSYS Static Structural analysis are applied in three steps and represent the real sequence of the cavity setup cycle. They are: pumping out of air inside of the cavity (applying an external pressure of 1 bar), installation of the inflatable gasket from the flat side of the flange (applying a pressure of 1.7 bar) and heating up the cavity (importing the temperature distribution from the Steady State Thermal).

Figure 5 represents the results after the last step. The magnitude of the resulting deformation reaches a maximum of 1.29 mm. Currently in progress, the second step of the mechanical design where the feedback of the structural deformation is included should answer the question of the tuning range.

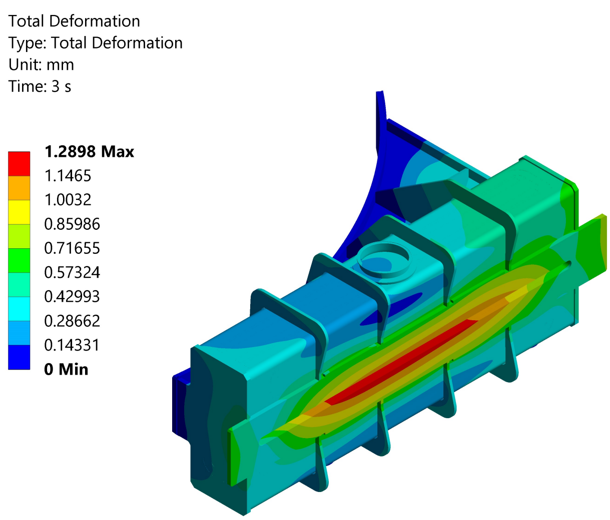

Figure 5: Total deformation of the new flat top cavity.

MULTIPACTING STUDIES

Probe measurements from the current flat top cavity have illustrated that there appears to be multipacting occuring on the original cavity back wall (see cavity back plane discoloration in Fig. 6). Using the Particle-in-Cell (PIC) solver from CST Studio's Suite [8], multipacting simulations were performed. It was possible to obtain similar crescent-shaped electron distributions when without the presence of the cyclotron static magnetic field maps (see Fig. 7). These simulations involve coupling the electromagnetic field maps generated by CST's eigenmode solver to the PIC solver. The cavity surfaces within the PIC solver settings were assigned a secondary emission yield curve of copper and aluminium, the values of which were taken from [9]. The source location of the electrons being unknown, an homogeneous electron distribution was assumed throughout a volume closed to the cavity back wall and comprising the electrodes' ends.

Applying identical settings, simulations were run for the new baseline geometry and for different electrode shapes. It was found that these crescent-shaped electron distributions were inherent to the cavity design even as the new cavity does not have the original cavity triangular-shaped reinforcements (see Fig. 6). Geometric changes of the back wall in the vicinity of the electrodes' ends and of horizontal middle cavity plane are being explored in order to remove the potential well which traps the particles between the four electrodes and the back wall.

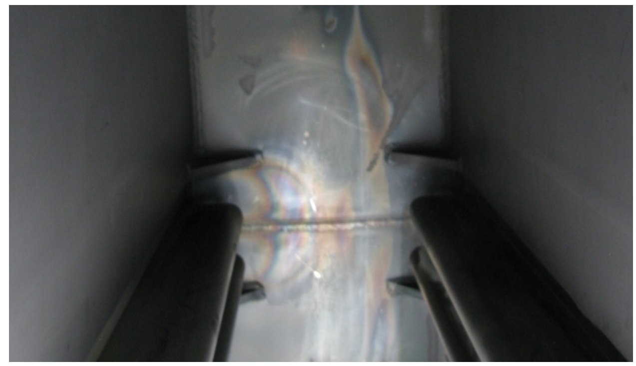

Figure 6: Back plane of the original cavity.

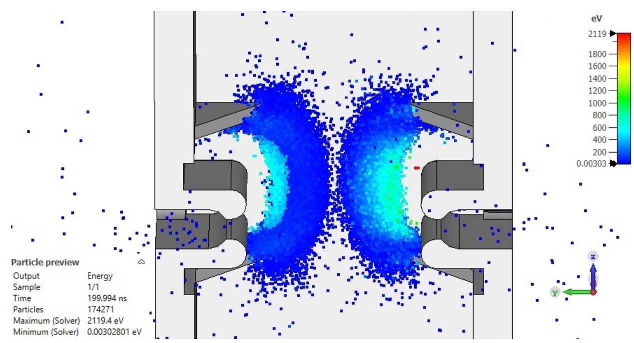

Figure 7: Multipacting simulations of the original cavity assuming copper material.

CONCLUSION

Designed to withstand a peak voltage of 700 kV and an average power of 140 kW, the RF design studies of the new 150-MHz flat top cavity show that adopting a horizontal distance between the electrodes of 250 mm and a maximum electrode thickness of 45 mm minimizes the required cavity dissipated power. Moreover, the modest dissipated power per electrode indicates that dedicated electrode cooling channels are not required. This new cooling channel system designed and simulated with ANSYS is such that the maximum cavity body does not exceed 70 °C. A one-way ANSYS Static Structural analysis of the cavity shows that the maximum structural deformation is less than 1.5 mm and self-consistent simulations are in progress. PIC CST Studio Suite multipacting studies have also been initiated by modifying the cavity back wall close to the electrodes' end.

ISBN: 978-3-95450-212-7 ISSN: 2673-5482 doi:10.18429/JACoW-CYCLOTRONS2022-WEPO018

REFERENCES

[1] L. Stingelin, M. Bopp, and H. Fitze, "Development of the new 50 MHz resonators for the PSI Injector II cyclotron", in *Proc. 18th Int. Conf. on Cyclotrons and their Applications (Cyclotrons'07)*, Giardini-Naxos, Italy, Oct. 2007, pp. 467-469.

[2] H. Fitze, M. Bopp, and H. Frei, "Development of a new high power cavity for the 590 MeV ring cyclotron at PSI", in *Proc. 1999 Particle Accelerator Conf. (PAC'99)*, New York, NY, USA, Mar.-Apr. 1999, paper MOP58, pp. 795-797.

[3] N. J. Pogue, L. Stingelin, and A. Adelmann, "Analysis and supression of RF radiation from the PSI 590 MeV cyclotron flat top cavity", *Nucl. Instrum. Methods Phys. Res. A*, vol. 828, pp. 156-162, 2016, doi:10.1016/j.nima.2016.05.026

[4] M. Bopp, H. Fitze, P. Sigg, and L. Stingelin, "Upgrade concepts of the PSI accelerator RF systems for a projected 3 mA operation", in *Proc. 16th Int. Conf. on Cyclotrons and their Applications (Cyclotrons'01)*, East Lansing, MI, USA, May 2001, paper P4-21, pp. 300-302.

[5] ANSYS HFSS, https://www.ansys.com/products/electronics/ansys-hfss

[6] ANSYS Workbench, https://www.ansys.com/products/ansys-workbench

[7] P. W. Dittus and L. M. Boelter, "Heat transfer in automobile radiators of the tubular type", *University of California Publications in Engineering*, vol. 2, no. 13, pp. 443-461, 1930. Reprinted in *Int. Comm. Heat Mass Transfer*, vol. 12, pp. 3-22, 1985.

[8] CST Studio Suite, https://www.3ds.com/products-services/simulia/products/cst-studio-suite

[9] V. Baglin *et al.*, "The secondary electron yield of technical materials and its variation with surface treatments", in *Proc. 7th European Particle Accelerator Conf. (EPAC'00)*, Vienna, Austria, Jun. 2000, paper THXF102, pp. 217-221.